Chemistry Africa (2022) 5:1527–1543
https://doi.org/10.1007/s42250-022-00402-8

ORIGINAL ARTICLE

Synthesis and Potential of Bio Fabricated Silver Nanoparticles for Use as Functional Material Against Foodborne Pathogens

Walla Alelwani[1] · Muhammad Babar Taj[2] · Reham M. Algheshairy[3] · Afnan M. Alnajeebi[1] · Hend F. Alharbi[3] · Azzah M. Bannunah[4] · Alaa Hamed Habib[5] · Ahmad Raheel[6] · Saima Shabbir[7] · Raja Hammad Ahmad[8] · Sadia Noor[9] · Mika Sillanpää[10,11]

Received: 15 December 2021 / Accepted: 6 June 2022 / Published online: 11 July 2022

Abstract

The discovery of antimicrobial agents continues to develop in line with advances in materials science and technology, and in light of resistance to many pathogens. Nanoparticle-based materials offer enhanced food preservation from foodborne pathogens. In this study, the simple, eco-friendly and non-toxic synthesis of silver nanoparticles (GC-AgNPs) by goat colostrum is reported for the first time. Confirmation of synthesized GC-AgNPs is based on UV–Visible and FTIR spectroscopy, scanning electron microscopy (SEM), and powder X-ray diffraction method (PXRD). The PXRD study confirms that GC-AgNPs are 6.93 nm in size. The role of goat colostrum proteins in the reduction of silver ions (Ag^{+}) to silver nanoparticles (AgNPs) is confirmed by FTIR analysis. The crystalline structure of the nanoparticles is determined by the XRD spectrum having characteristic peaks at (111), (200), (220), and (311) respectively, correlated with silver Bragg reflections. The antimicrobial potential of GC-AgNPs is studied using multiple bioassays. GC-AgNPs exhibit 93% DPPH scavenging activity. The antioxidant results of various bioassays show that GC-AgNPs have a strong ability to stabilize the oxidized metal ions and can accept the electron in anaerobic and anhydrous conditions. GC-AgNps represent the highest inhibition zone (40.27 mm) for *Pseudomonas Aeruginosa* and *Aspergillus flavus* (18.34 mm) and are highly biocompatible as cleared from their cytotoxicity ($IC_{50} = 615 \pm 0.64$ mg/mL) against L-929 fibroblast cell lines. Therefore, it can be concluded that non-toxic and antimicrobial GC-AgNPs may be used as potential antimicrobial agents against foodborne pathogens.

Walla Alelwani and Muhammad Babar Taj have equal contribution and may please be considered as first authors.

✉ Muhammad Babar Taj
dr.taj@iub.edu.pk

✉ Mika Sillanpää
mika.sillanpaa@tdtu.edu.vn

1 Department of Biochemistry, College of Science, University of Jeddah, Jeddah, Saudi Arabia

2 Institute of Chemistry, The Islamia University Bahawalpur, Bahawalpur 63100, Pakistan

3 Department of Food Science and Human Nutrition, College of Agriculture and Veterinary Medicine, Qassim University, Buraydah 51452, Saudi Arabia

4 Department of Basic Sciences, Common First Year Deanship, Umm Al-Qura University, Makkah, Saudi Arabia

5 Department of Physiology, Faculty of Medicine, King Abdulaziz University, Jeddah 21589, Saudi Arabia

6 Department of Chemistry, Quaid-e-Azam University, Islamabad 44000, Pakistan

7 Department of Materials Science and Engineering, Institute of Space Technology, Islamabad 44000, Pakistan

8 Department of Nano Science and Technology, National Centre for Physics, Islamabad 44000, Pakistan

9 Department of Chemistry, University of Agriculture, Faisalabad 38000, Pakistan

10 Environmental Engineering and Management Research Group, Ton Duc Thang University, Ho Chi Minh City, Vietnam

11 Faculty of Environment and Labour Safety, Ton Duc Thang University, Ho Chi Minh City, Vietnam

Graphical Abstract

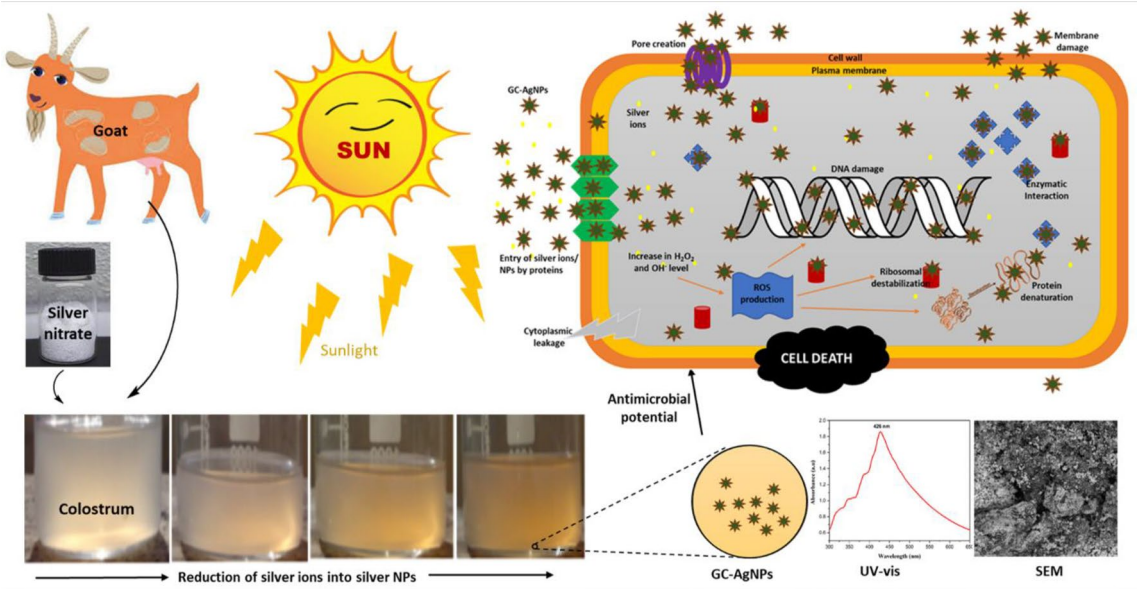

Keywords Silver nanoparticles · Milk proteins · Antimicrobial activities · Foodborne pathogens

1 Introduction

Microbial contamination is a prevalent concern in food processing. Scientists employ metal nanoparticles like silver, and gold dioxide, magnesium oxide, zinc oxide, copper oxide, cadmium selenite/tellurite, and titanium to cope with microbial activities. Nanoparticles exhibit some exceptional and novel properties depending on their size, shapes, and morphological attributes, endorsing their interactions with animals, plants, and microorganisms [1–3]. They are prepared to investigate their physical properties and morphological features from different perspectives [1, 4–8]. Numerous factors determine the stability, size, and morphological attributes of nanoparticles, particularly the synthetic protocol, solvent, temperature, concentration, and strength of the reducing agent [9]. Some researchers mistakenly claimed that the chemical synthesis of nanoparticles is green, although it was done inadvertently [10].

It is well known that green synthesis involving biological materials provides the best environmental platform for reducing the metal ions into metallic nanoparticles [11–15]. In recent times, gold and silver nanoparticles have been synthesized from floral parts, fruits, and leaves of plants [1, 9, 16–18], apart from typical enzyme-based synthesis [19]. The AgNPs have gained a significant position among all previously reported nanoparticles owing to their inherent antimicrobial property, even in the solid-state [20–27]. The synthesis of nanoparticles using various animal milk like camel milk, sheep milk and goat milk has already been reported by a few researchers e.g., Akshata et al. [28] used milk in an orbital shaker at 37 °C, 120 rpm for 72 h and Pandey et al. [29] used milk at 60 °C to synthesize AgNPs. The milk proteins reduce the metal ions and stabilize the nanoparticles [29] and it is also expected that at high-temperature casein and whey proteins interact with each other to result in abnormal functional properties [29, 30]. Still, the mechanism and use of proteins in the synthesis of AgNPs have not been much investigated. Only Lee et al. [31] and Hegazi et al. [32] reported the significant antimicrobial activity of cow milk mediated silver nanoparticles. So, there is still a need for new antimicrobial materials to overcome existing microbial resistance challenges.

Although milk is already used in the synthesis of silver nanoparticles, no studies regarding goat colostrum have been reported. Colostrum is the milk, which is produced right after calving. It is rich in proteins, antibodies and amino acids relative to common breast milk, which start to appear after the first day of calving [33]. In this study, we used goat colostrum for the first time to synthesize GC-AgNPs from a silver salt solution. We have thoroughly examined the antimicrobial potential of GC-AgNPs through various biological activities such as (i) DPPH radical scavenging assay, (ii) metal chelation assay, (iii) phosphomolybdenum assay, (iv) azinobis 3-ethylbenzothiazoline-6-sulfonate ($ABTS^{\cdot+}$) assay, (v) hydrogen peroxide (H_2O_2) scavenging assay, (vi) nitric oxide radical scavenging assay, (vii) reducing power assay,

(viii) antibacterial disk diffusion assay, (ix) antibacterial disk diffusion assay, (x) time course growth assay, (xi) Broth dilution (BD) method, (xii) anti-inflammatory assay, and (xiii) biocompatibility assay.

2 Material and Methods

2.1 Materials

GC-AgNPs were synthesized by utilizing the following precursors; Silver nitrate ($AgNO_3$, 99.99% Sigma-Aldrich); Ammonium molybdate ($(NH_4)_2MoO_4$, 99.99% Sigma-Aldrich); Sodium Phosphate (NaOH, 98% Sigma-Aldrich); Potassium persulfate ($K_2S_2O_8$, 99.99% Sigma-Aldrich); Sulphuric Acid (H_2SO_4, 98% Sigma-Aldrich); Ethylenediaminetetraacetic acid (EDTA, 99.98% Sigma-Aldrich); Hydrogen peroxide (30 wt % in H_2O Sigma-Aldrich); All chemicals were used as received.

2.2 Synthesis of Silver Nanoparticles (GC-AgNPs)

The goat colostrum mediated silver nanoparticles were prepared by adding 5 mL fresh goat colostrum to 50 mL of 10^{-4} M $AgNO_3$ aqueous solution for reducing Ag^+ ions. This reaction mixture was kept in direct sunlight for two days and the formation of silver nanoparticles from the reduction of silver ions was confirmed when the white colour of goat colostrum changed to reddish-brown. The nanoparticles were collected after centrifugation and finally purified using distilled water. The unbound proteins were removed with 80% ethanolic solution (v/v).

2.3 Characterization of Silver Nanoparticles

The synthesized GC-AgNPs (obtained from the bio-reduced Ag^+ ions) in the medium were monitored through a UV–Visible spectrophotometer (Lambda-35 R PerkinElmer, USA) in the 300–650 nm wavelength range. The spectra were monitored w.r.t., time at a 1 nm resolution, and ambient temperature.

The diameter of the nanoparticles was determined at a fixed scattering angle of 90° and ambient temperature. FT-IR spectra of GC-AgNPs have been recorded on Fourier Transform Infra-Red spectrophotometer (FTIR; 8400S, Shimadzu, Japan) with transmission (%) mode and 200 scans. For FT-IR analysis, potassium bromide KBr-pelletized, GC-AgNPs having 1% (w/w) concentration were compared with pure KBr pellet as a reference background. The morphological structure analysis and the size of silver nanoparticles were performed on scanning electron microscopy (SEM) (Model No: Jeol 6480LV; JSM, USA) keeping acceleration voltage at 15 kV.

2.4 Biological Activities Against Foodborne Pathogens

2.4.1 Antioxidant Activities

2.4.1.1 DPPH Radical Scavenging Assay The DPPH radical scavenging activity of GC-AgNPs was investigated using the reported method [34] with some modifications. Various concentrations of GC-AgNPs (10, 10, 20, 30, 40, 50, 75, and 100 µg/mL) and butylated hydroxytoluene (BHT) were transferred to sample test tubes and 5 mL of ethanolic DPPH solution (0.1 mmol/L) was added by vigorous shaking. The sample tubes were placed in the dark ambient for about 30 min. The activity was assessed by taking absorbance at 517 nm. The DPPH radical percent inhibition was calculated using the optical density (OD) of the samples and the control using Eq. 1 as given below.

$$DPPH\ percent\ inhibition(\%) = \frac{(OD\ of\ control - OD\ of\ sample)}{OD\ of\ control} \times 100. \quad (1)$$

2.4.1.2 Metal Chelation Assay The GC-AgNPs were also tested for chelation activity with ferrous ions by following a reported method [35]. In the first step of process, different concentrations of the GC-AgNPs (100, 200, 300, 400 and 500 µg/mL) and 0.1 mL of $FeCl_2$ solution (2 mmol/L) were mixed. To initiate the chelation reaction, ferrozine solution (0.2 mL; 5 mmol/L) was mixed in the reaction medium and by vigorous and continuous shaking and then kept at ambient temperature for almost 10 min. Afterwards, the absorbance was measured at 562 nm to calculate the Fe^{2+} ion's chelating activity. Ethylenediaminetetraacetic acid (EDTA) as a standard was used to measure the chelation activity of the GC-AgNPs. The chelating activity is expressed in milligrams of EDTA equivalent/gram of sample. The percent inhibition (%) of ferrozine–Fe^{2+} complex was computed with the help of the following Eq. 2.

$$Fe^{2+}\ ions\ chelating\ activity\ (\%) = \left[A_{control} - A_{sample/standard}\right] \times 100. \quad (2)$$

2.4.1.3 Phosphomolybdenum Assay The antioxidant potential of the GC-AgNPs was also evaluated against phosphomolybdenum following a reported procedure [36]. The sample vial was loaded with reagent solution [prepared by mixing, sodium phosphate (4 mM), ammonium molybdate (4 mM) and sulfuric acid (0.6 M)], and sample solution (100, 200, 300, 400 and 500 µL respectively). The capped sample vials were incubated in a thermostat at 95 °C for 90 min. On attaining room temperature, the absorbance of samples

was recorded at 695 nm to measure phosphomolybdenum antioxidant activity as ascorbic acid equivalents (AAE/g).

2.4.1.4 Azinobis 3-Ethylbenzothiazoline-6-Sulfonate ($ABTS^{\cdot+}$) Assay The GC-AgNPs were also assessed for their ABTS radical cation ($ABTS^{\cdot+}$) decolourization activity, following a reported method [37]. The radical cations ($ABTS^{\cdot+}$) were produced by reacting aqueous azinobis 3-ethylbenzothiazoline-6-sulfonate $ABTS^{\cdot+}$ solution (7 mM) with potassium persulfate (2.4 mM), in the dark in a room temperature for almost 12–16 h. Ethanol (approximately 1:89 v/v) was used for diluting the reagent solution and subsequently equilibrated at 30 °*C* to measure the absorbance (0.7 ± 0.02) at 734 nm. To the samples of varying concentrations (100, 200, 300, 400, and 500 µg/mL), 3 mL of $ABTS^{\cdot+}$ reagent (0.1 mM) was added and kept in the dark place to incubate for 15 min. The absorbance was measured at 745 nm to assess the extent of decolourization. Rutin was the standard and ABTS reagent was designated as the control. The percent $ABTS^{+}$ inhibition was calculated with Eq. 3.

$$ABTS\ inhibition\ (\%) = \frac{(The\ absorbance\ of\ the\ control - absorbance\ of\ the\ sample)}{The\ absorbance\ of\ the\ control} \times 100. \quad (3)$$

2.4.1.5 Hydrogen Peroxide (H_2O_2) Scavenging Assay The silver nanoparticles were also assayed with Hydrogen peroxide (H_2O_2) scavenging activity by slight modification in the previously reported assay [38]. The method is briefly described here; 50 mL of H_2O_2 (5 mM) solution was added to the GC-AgNPs of varying concentrations (10 20, 30, 40, 50, 75, and 100 g/mL) and standard ascorbic acid. The reaction mixtures were incubated at ambient conditions for 20 min and afterwards, the absorbance of solutions was measured at 610 nm. The scavenging activity was determined from Eq. 4.

$$Scavenging\ activity(\%) = \frac{(The\ absorbance\ of\ the\ control - absorbance\ ofthe\ sample)}{The\ absorbance\ of\ the\ control} \times 100. \quad (4)$$

2.4.1.6 Nitric Oxide Radical Scavenging Assay This scavenging activity was determined from nitric oxide radicals ($NO^{\cdot}$), generated by the interaction of oxygen with aqueous sodium nitroprusside solution (100 µL of 20 mM) at physiological pH. The nitrite ions were measured with Griess reagent after slight modification in the protocol reported by Sousa [39]. The incubation of nitric oxide radicals with 100 µg/mL of GC-AgNPs was carried out for an hour under ambient conditions. Commercial phenolic BHT and $NO^{\cdot}$ were the positive controls in this assay and scavenging activity was calculated from the same Eq. 4.

2.4.1.7 Reducing Power Assay The GC-AgNPs were investigated for their reducing power using a slight modification in the reported protocol [40]. In this method, the solutions of GC-AgNPs in varying concentrations (10, 20, 30, 40, 50, 75 and 100 µg/mL), phosphate buffer (2.5 mL of 200 mM; pH 6.6) and potassium ferricyanide (2.5 mL of 1%) were mixed. The reaction mixture was incubated at 50 °C for 20 min and suddenly cooled and TCA solution (2.5 mL of 10%) was added. The reaction mixture was centrifuged at 3000 rpm for 8 min. Afterwards, the supernatant and Millipore Milli-Q water were mixed in equal amounts. Finally, a $FeCl_3$ reagent (1 mL of 0.1%) was added to the upper layer of the supernatant and measured the absorbance of samples at 700 nm. The results were compared with positive control and the percent reducing power was calculated with Eq. 4.

2.4.2 Antimicrobial Assay

2.4.2.1 Antibacterial Disk Diffusion Assay For this assay, sterile agar plates were prepared using 20 mL of sterile nutrient agar liquid medium (pH 7.4 ± 0.2). Once we attained the solidification of plates, the bacterial sample containing 100 µL of suspension (10^5 colony-forming units/mL) was applied to the agar plates. The suspended solutions (5 mg/mL, 10 mg/mL) of $AgNO_3$ and the GC-AgNPs were impregnated on sterile disk filter paper (6 mm in diameter). Disks loaded with samples were afterwards positioned on inoculated agar plates. The sensitivity of bacterial species to GC-AgNPs was determined using positive control chloramphenicol (10 mg/mL). The inoculated plates were incubated for 24 h keeping the thermostat at 37 °C. Antibacterial activity was assessed from inhibition zones [41].

2.4.2.2 Antifungal Disk Diffusion Assay The antifungal activity of $AgNO_3$ and the GC-AgNPs was determined by the disk diffusion method [42]. The point inoculation method was used to inoculate potato dextrose agar plates with 10 days old fungal cultures. Disk filter papers (Whatman No. 1) impregnated with $AgNO_3$ and the GC-AgNPs (5 and 10 mg/mL), were placed on test organism seeded agar plates. Nystatin (10 mg/mL) was the positive control in this assay. The antifungal activity was determined after incubating the samples for 72 h at 28 °*C*. The inhibition zones were located and their diameters, as well as mean values, were determined with a calliper.

2.4.2.3 Time Course Growth Assay The sensitivity of GC-AgNPs and $AgNO_3$ for pathogenic bacterial strains was measured by time course growth assay [43]. From the bacterial culture incubated overnight in a nutrient broth (NA), 100 µL was put into sterile test vials loaded with 1 mL of NA and 100 µL of $AgNO_3$/ GC-AgNPs (5 mg/mL, 10 mg/mL). The inoculated sample in the tubes was thoroughly mixed and incubated at 37 °C. The optical density (OD) of samples was measured at 550 nm on a micro quant spectrophotometer (BioTek; USA) after time intervals of 0, 1, 2, 3, and 5 h. The bacteriostatic effect of incubated cultures led to a decrease in optical density. Three technical replicates of the assay were taken.

2.4.2.4 Broth Dilution (BD) Method Minimum Inhibition Concentration (MIC): The visible growth of microorganisms in Mueller–Hinton, MH (for bacteria) and Sabouraud dextrose, SD (for fungi) broth was evaluated in terms of minimum inhibition concentration (MIC) and Minimum Bactericidal Concentration (MBC). 100 µL of GC-AgNPs (200 to 1 µg/mL) was poured into microtitre plates with 100 µL each broth. After two-fold serial dilution, 100 µL of microbial samples were incubated for 24 h (for bacteria) and 48 h (for fungi) at 37 °C [44]. The optical densities were calculated at 600 nm using a microplate reader.

Minimum Bactericidal Concentration (MBC) and Minimum Fungicidal Concentration (MFC): To calculate MBC and MFC, 2 µL of microbial sample from MIC well were incubated for 24 h and 48 h respectively at 37 °C. The point where silver nanoparticles kill 99.9% of the microbial population is called the MBC (bacteria) and MFC (fungi) point [45].

2.4.3 Anti-inflammatory Assay

The GC-AgNPs were testified for their anti-inflammatory potential using albumin denaturation protocol [46]. In this method, the reaction mixture was prepared by mixing 0.2 mL of fresh egg albumin (hen's egg), 2.8 mL of PBS (pH 6.4), and 2 mL of GC-AgNPs (25, 50, 100, 200, and 400 µg/mL). The reaction mixture was placed in a BOD incubator for 15 min initially at 37 °C and then the temperature was raised to 70 °C for 5 min. The distilled water was taken as control. The absorbance of the sample was measured at 660 nm after cooling it to room temperature. The reference drug acetylsalicylic acid of varying concentrations (5, 10, 15, 25, 50, and 100 mg/mL) was prepared as the abovementioned procedure and absorbance was measured. The inhibition of denaturation was calculated with the following Eq. 5.

$$Inhibition\ (\%) = 100 \times \frac{V_t}{V_c}. \tag{5}$$

where V_t is the absorbance of the test sample and V_c stands for the absorbance of the control. The IC_{50} (the concentration of drug causing 50% inhibition of denaturation), was determined from the dose/ response curve by plotting percent inhibition of control against varying concentrations of treatment.

2.4.4 Biocompatibility Study

The GC-AgNPs were also evaluated for their biocompatibility from the percent viability of normal fibroblast cell lines (L-929) [46]. The seeding of L-929 cells was carried out in a flask containing Dulbecco's modified Eagle's medium (DMEM) and M-199 supplemented with fetal bovine serum FBS (10%) and incubated for one day under a 5% CO_2 atmosphere at 37 °C. After incubation, intact cells were trypsinized for about 3–5 min to separate individual cells and then centrifuged at 800 rpm for 10 min. The number of individual cells was estimated and 5000 cells/well were distributed in a 96-well ELISA plate and incubated for 24 h until 70–80% convergence of monolayer. The remarkable capacity of GC-AgNPs to reduce the ATPs of the cells ultimately caused mitochondrial damage and a dose-dependent increment of reactive oxygen species (ROS). Hence, the GC-AgNPs of concentrations ranging from 100 to 700 mg/mL were tested for toxicity. The viability of the cells was detected after adding 200 mL of MTT solution (3-(4,5-dimethylthiazol-2-yl)-2,5-diphenyltetrazolium bromide) to sample wells and incubating for 4–5 h. Afterwards, 200 mL of DMSO was transferred to the wells discarding the MTT solution and kept in dark for almost 15–20 min. Post-incubation optical density (OD) of the formazan product was measured on a micro-titre plate reader at 595 nm.

2.4.5 Statistical Analysis

All bioactivity assays were run in triplicates to ensure their reproducibility. The results of antioxidant activities were expressed in percent inhibition (%) while the cytotoxic activity was expressed in percent viability as compared to control. The comparison of antioxidant and cytotoxic activities was made with the "Student's t-test" with the respective controls. The collected data were then subjected to one-way ANOVA and Duncan's Multiple Range Test processed on the SPSS program (IBM SPSS; statistics 19). A statistical difference was considered significant at $p \leq 0.05$.

3 Results and Discussion

3.1 Synthesis of GC-AgNPs

Silver nanoparticles have been reported for their penetrating potential in biomedical applications [47]. The controlled magnitude of silver nanoparticles was herein accomplished with an appropriate quantity of goat colostrum. The colostrum contains a high concentration of proteins and a low concentration of fat (see Supplementary Material). The appearance of reddish-brown colour indicated the formation of elemental silver (Ag°) from silver ion (Ag^{+}) reduction and surface plasmon resonance of the newly synthesized GC-AgNPs triggered this process. The GC-AgNPs presented noteworthy biomedical applications in terms of antioxidant, antimicrobial, antifungal, and anti-inflammatory activities.

3.2 UV–Visible Spectroscopy

The UV–Vis analysis of GC-AgNPs endorsed their visual results and stabilization at 426 nm (Fig. 1), which is in close agreement with the wavelength of surface plasmon resonance in silver. The investigation revealed that the overall yield and growth of the GC-AgNPs are greatly influenced by various factors including sliver salt's concentration, precursors, and goat colostrum. In this study, we employed 1–5 mM $AgNO_3$ salt at ambient reaction conditions, and strong absorbance at 426 nm due to the formation of GC-AgNPs. The surface plasmon vibration caused a sharp absorbance between 410 and 440 nm, which is mainly due to the enriched concentration of silver nanoparticles, as reported in the literature [48–51].

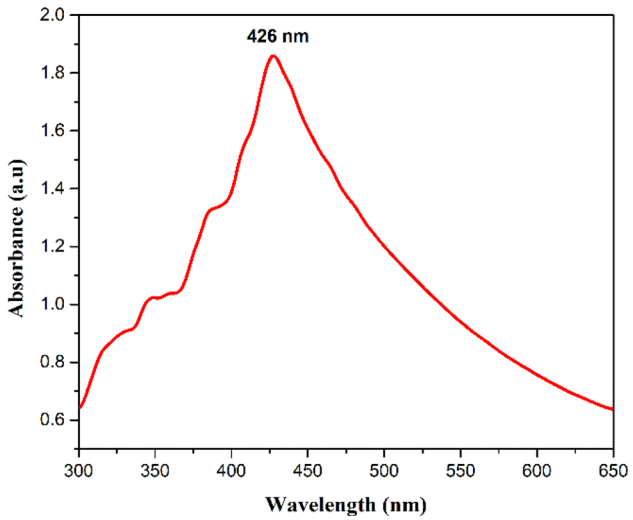

Fig. 1 UV visible spectrum of GC-AgNPs

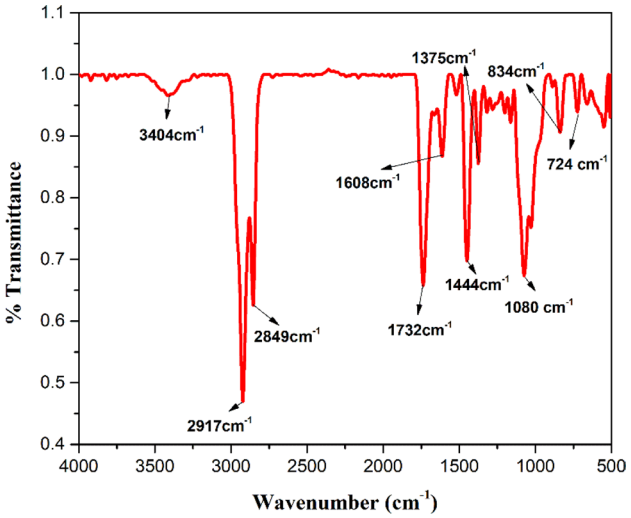

Fig. 2 FTIR spectrum of GC-AgNPs

3.3 FTIR Spectroscopy

The biosynthesis methods significantly enhanced the stability of nanoparticles, as bio-functionalization confers stability. The FTIR spectrum (Fig. 2) of the GC-AgNPs synthesized from goat colostrum on exposure to direct sunlight showed the characteristic peaks, observed at 3404, 2917, 2849, 1732, 1608, 1444, 1375, 1080, 834, 724 cm^{-1} in clear comparison to the peaks in FTIR spectrum of goat colostrum spectrum (Supplementary material Fig S1).

3.3.1 Plausible Mechanism

It is presumed that the proteins and enzymes in the goat colostrum confer characteristic absorption peaks which in turn may be the causative agents to accelerate reduction and capping. Sunlight provides sufficient energy to accelerate the biomolecules to fabricate nanoparticles [52, 53]. The presence of the hydroxyl group or secondary amine was identified at 3404 cm^{-1}. A characteristic band at 1608 cm^{-1} in FTIR spectra is assigned to amide I. It can be inferred from the FTIR analysis that the stretching vibrations of –C=O and –N–H in the proteins of colostrum cause the reduction and the functionalization of GC-AgNPs. The peaks spotted at 1375 cm^{-1} and 1444 cm^{-1} account for the C-N stretching vibrations of amide II and amide III correspondingly. It can be deduced from the abovementioned analysis; that photoreduction of Ag^{+} to AgNP is directly influenced by the proteins in goat colostrum. The peak observed at 2917 cm^{-1} represents the *str* vibrations of $–CH_3$ and at 2849 cm^{-1} represents $–CH_2$. The strong and sharp peak at 1732 cm^{-1} is linked to the propionamide side chain of Vitamin B_{12} present in the goat colostrum [54, 55]. It also provides an understanding that the colostrum proteins could be adsorbed on

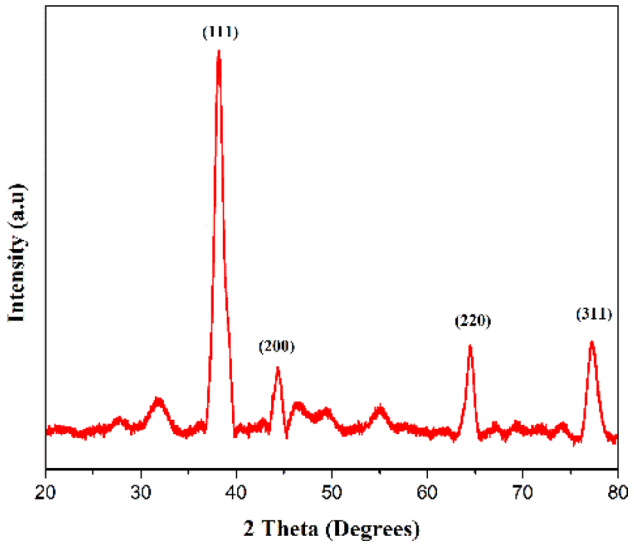

Fig. 3 PXRD pattern of GC-AgNPs

the metal surface along with Vitamin B_{12}. Hence it is conferred that the presence of proteins in the goat colostrum facilitates the photocatalytic synthesis of the GC-AgNPs from Ag^{+} ions.

3.4 Phase and Crystallinity Analysis

The crystalline nature of GC-AgNPs was confirmed by X-ray diffraction (XRD) analysis, and the XRD pattern revealed numbers of Braggs reflections indexed based on face centred cubic structure of silver. The nanocrystal structure of GC-AgNPs was confirmed by the analogy of our XRD spectrum (ref no. 01-087-0719) to that of standard, as verified by the appearance of peaks at 2θ values of 38.3° (111), 44.1° (200), 64.6° (220), and 77.2° (311) corresponding to the Bragg reflections of silver [56] (Fig. 3). As elaborated in the experimental section, the synthesized nanoparticles were repeatedly centrifuged and dispersed in distilled water before the XRD analysis to prevent Bragg reflections caused by independent crystallization of any unbound biological material. The average particle size of GC-AgNPs was 6.93 nm, calculated by using the Debye-Scherer Equation [57].

3.5 Morphological Analysis

The morphological attributes, shape, and size of the GC-AgNPs were clarified by employing Scanning Electron Microscopy (SEM). The SEM image (Fig. 4) confirmed that the nanoparticles appeared with sizes of 45.96–64.88 nm having an average size of 55.42 nm. This range of particle size could be due to the aggregation of smaller particles or the overlapping capping agents. The aggregated GC-AgNPs endorsed the synthesis of silver nanoparticles and their capping through the biomolecules especially proteins in goat colostrum.

3.6 Evaluation of Biological Activities Against Foodborne Pathogens

3.6.1 Antioxidant Activities

3.6.1.1 DPPH Radical Scavenging Activity The DPPH is a stable free radical, known for its ability to accept hydrogen

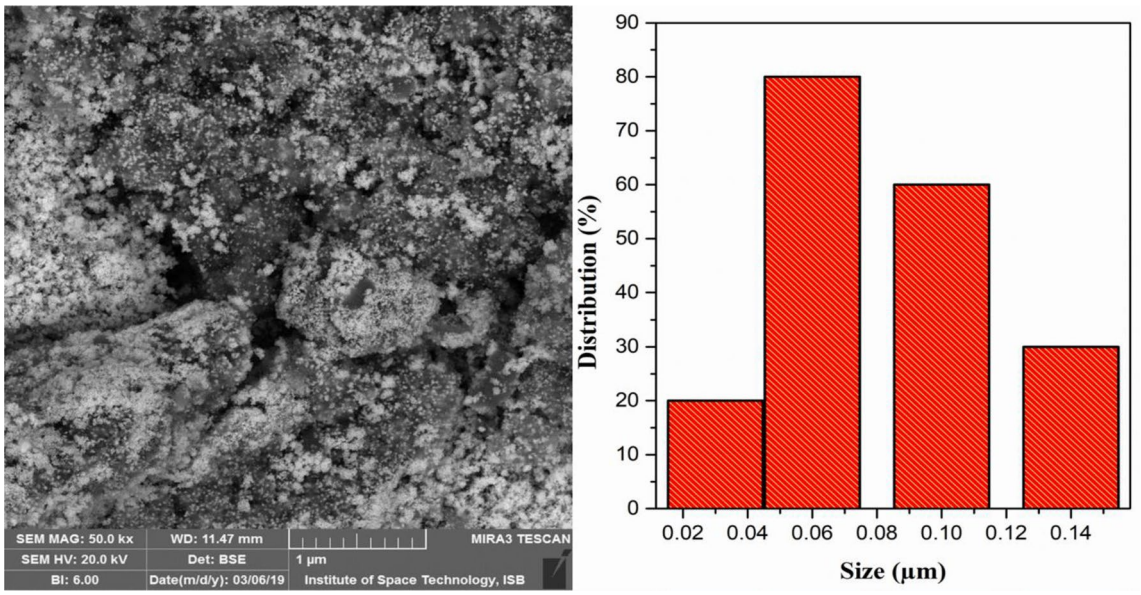

Fig. 4 SEM and histogram of GC-AgNPs

or electrons from donors. The DPPH reducing the ability of the GC-AgNPs was determined by the change in colour due to the donation of hydrogen to stable DPPH molecule, on the contrary; the control showed no colour change. There was considerable inhibition of GC-AgNPs against DPPH as compared to the BHT standard (Fig. 5). The dose-dependence increment of the GC-AgNPs in DPPH activity was observed. However, 93% scavenging activity of DPPH was exhibited by the GC-AgNPs. The absorbance was recorded at 517 nm in this assay. This antioxidant potential of the GC-AgNPs could be ascribed to the adherence of characteristic functional groups originating from the goat colostrum.

3.6.1.2 Chelation Activity Iron is an active catalyst and pro-oxidant to oxidize lipids. It accelerates the oxidation in its ferrous state by breaking down lipid peroxides and hydrogen to generate highly reactive free radical species. Ferrozine can form Fe^{2+}-complexes in quantitative amounts and the presence of other chelating agents, disrupt complexation. The highest metal chelation activity shown by EDTA is 99.27% ± 1.84 (Fig. 6). The Fe^{2+} ion chelating ability of synthesized GC-AgNPs is 68.56% ± 2.68 compared with previous results. In short, the chelating agents are the secondary antioxidants, that stabilize the metal ions in their oxidized forms and cause a reduction in their redox potential.

3.6.1.3 Phosphomolybdenum Activity The phosphomolybdenum assay gives a quantitative estimation of the antioxidant potential of synthesized GC-AgNPs and measures Mo(VI) to Mo(V). The reducing activity was indicated by the appearance of the green phosphate-Mo(V) complex and showed absorbance at 695 nm. The present study revealed that the GC-AgNPs showed phosphomolybdenum reduction activity (85 µg/mL) (Fig. 7). It is noted that the structure of the antioxidant understudy is responsible for the transfer of electrons at different redox potentials during the chelation process and phosphomolybdenum assay.

3.6.1.4 Azinobis 3-Ethylbenzothiazoline-6-Sulfonate ($ABTS^{\cdot+}$) Activity Another useful technique "$ABTS^{\cdot+}$ assay helps in determining the antioxidant potential of aqueous phase radicals (hydrogen donating antioxidants) and the lipid peroxyl radicals (chain-breaking antioxidants). Significant free radical inhibition was shown by the synthesized GC-AgNPs and the activity increased by increasing concentration. The maximum inhibition shown by GC-AgNPs is 89% at 500 µg/mL which is greater than the standard rutin (73%) as shown in Fig. 8.

3.6.1.5 H_2O_2 Scavenging Measurements In the biological systems, the membranes suffer huge damage by an uninhibited accumulation of H_2O_2 as oxygen free radicals (perox-

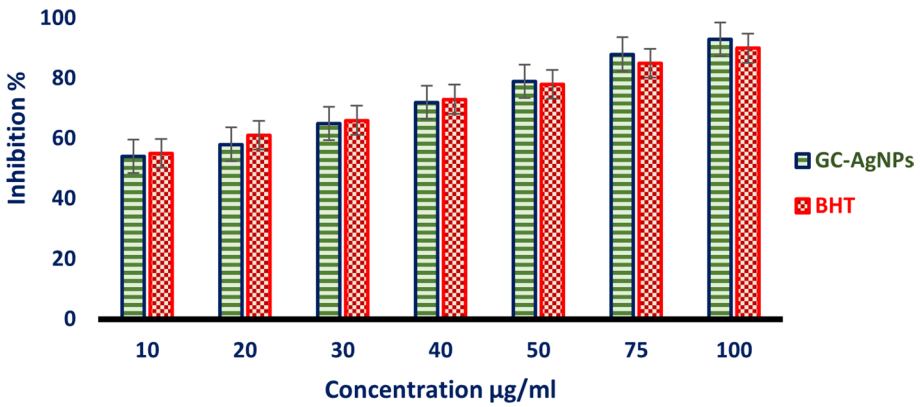

Fig. 5 DPPH radical scavenging activity of GC-AgNPs

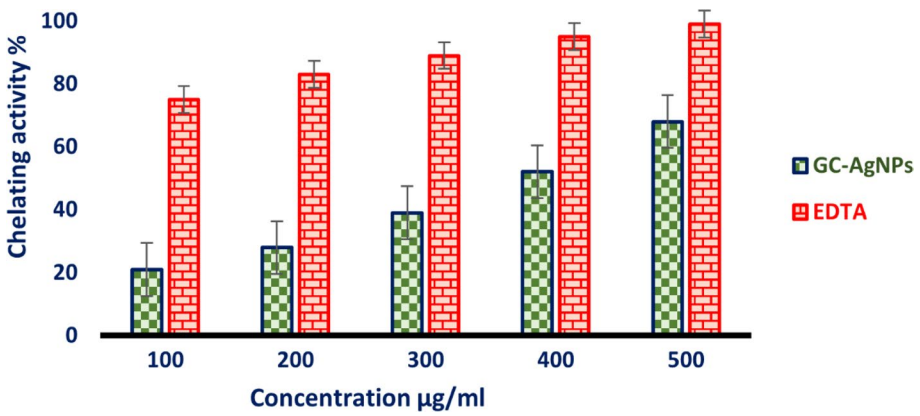

Fig. 6 Metal chelation activity of GC-AgNPs

ide and hydroxyl radicals) are generated in the process. The GC-AgNPs were evaluated spectrophotometrically for their quantitative H_2O_2 scavenging activity with standard antioxidant ascorbic acid as depicted in Fig. 9. At the highest concentration (100 µg/mL), the GC-AgNPs showed 94.12% inhibition in comparison to 90.28% inhibition of ascorbic acid. Interestingly, the free radicals generated during the H_2O_2 scavenging assay were higher than those in the DPPH scavenging assay. Surprisingly, the characteristic structural attributes of GC-AgNPs enhanced their reducing potential in comparison to ascorbic acid. The dispersed GC-AgNPs can trigger the formation of hydroxyl radicals in the presence of hydrogen peroxide, and hence their dissolution is accelerated due to the maximal incorporation of hydrogen peroxide inside the cell. This triggers strong oxidative stress even at a low dose. GC-AgNPs induce greater inflammasome formation due to greater involvement of hydrogen peroxide and cause efflux of K^+ ions and leakage of cathepsins

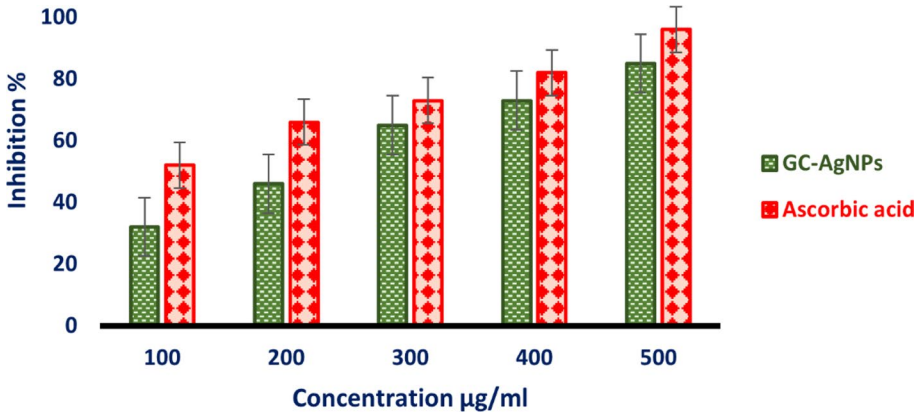

Fig. 7 Molybdenum reduction activity of GC-AgNPs

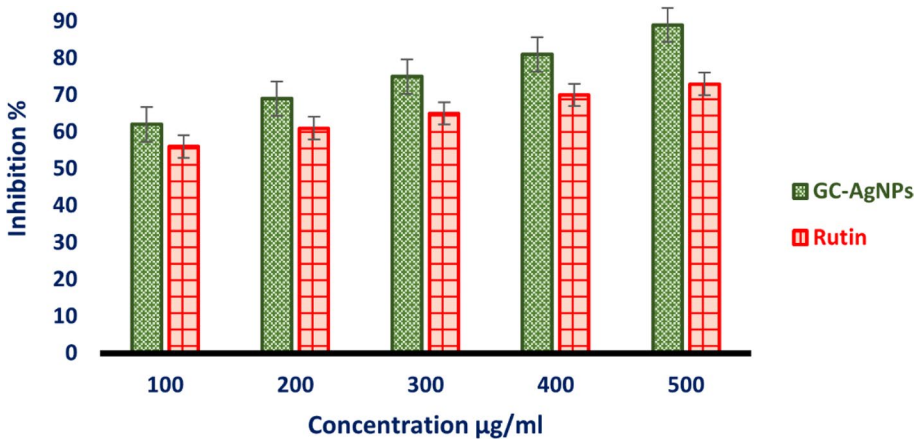

Fig. 8 $ABTS^{\cdot+}$ activity of GC-AgNPs

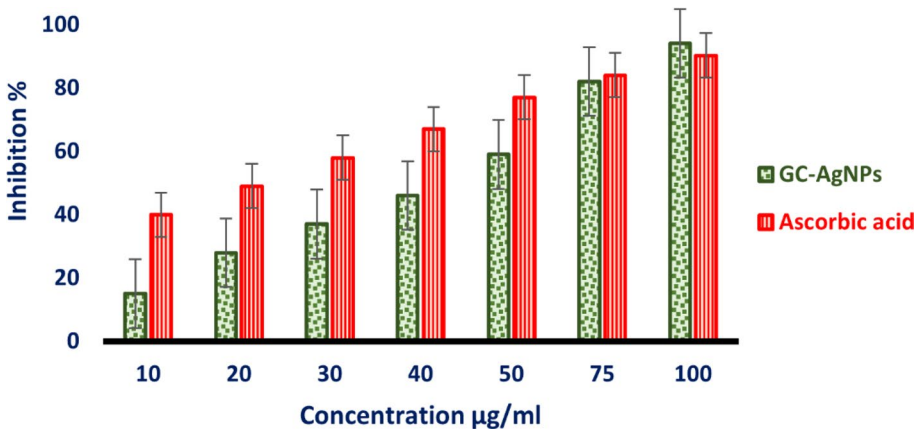

Fig. 9 H_2O_2 scavenging activity of GC-AgNPs

from impaired lysosomes. This process may be a major contributor to producing hydrogen peroxide and superoxide in the mitochondrial membranes.

3.6.1.6 Nitric Oxide Scavenging Activity Nitric oxide (NO) has been reported for many significant bioregulatory functions in the cardiovascular, immune, and nervous systems. The NO scavenging activity was concentration-dependent and the highest scavenging activity (80.02%) of the synthesized GC-AgNPs was observed at the highest concentration (100 mg/mL) (Fig. 10). The experimental findings clearly showed that NO activity was lower as compared to standard BHT (81.35%). The less stable NO radical has a high electronegativity, and it interacts at room temperature with GC-AgNPs under anaerobic and anhydrous conditions to accept electrons.

3.6.1.7 The Reducing Power The reducing power of the GC-AgNPs was determined from the dose-dependent response as graphically represented in Fig. 11. An increasing trend in the reducing power of the GC-AgNPs was observed with increasing concentrations. The involvement of biomolecules in goat colostrum improved the reducing power of the nanoparticles more than standard BHT. Nevertheless, the biomolecules of quol (polyphenolic daidzein metabolite) exhibit better antioxidant capacity in correlation to the synthesized GC-AgNPs.

3.6.2 In-Vitro Antimicrobial Potential

3.6.2.1 Disk Diffusion Antibacterial Activity The inhibition shown by gram-positive bacterial strains (*Bacillus tropicalis, Staphylococcus aureus*) and gram-negative bacterial strains (*E. coli and Pseudomonas aeruginosa)* was very significant (Table 1).

The GC-AgNPs and $AgNO_3$ treatments showed inhibitory zones of diameters of 40.27 mm and 12 mm respectively (Table 1). When the GC-AgNPs and $AgNO_3$ (10 mg each) were treated against *P. Aeruginosa*, the highest inhibition zones were observed at 40.27 mm and 26 mm, respectively. The same treatment with 5 mg each of the GC-AgNPs and $AgNO_3$ showed correspondingly zones at 31.7 mm and 25 mm. Among these treatments, inhibitory zones of $AgNO_3$ (5 mg) were observed in the range of 10.04–26.00 mm. Moreover, in the treatment with GC-AgNPs (10 mg) with *E. coli* and *Bacillus subtilis*, the respective inhibitory zones

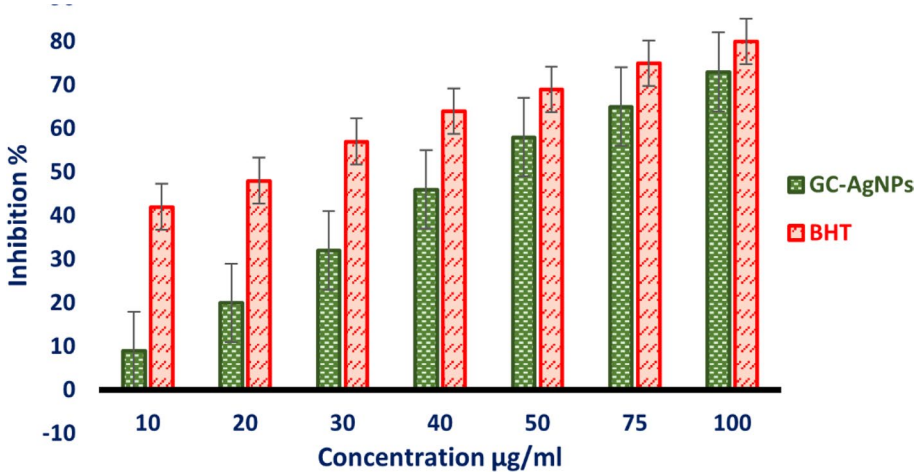

Fig. 10 Nitric oxide scavenging activity of GC-AgNPs

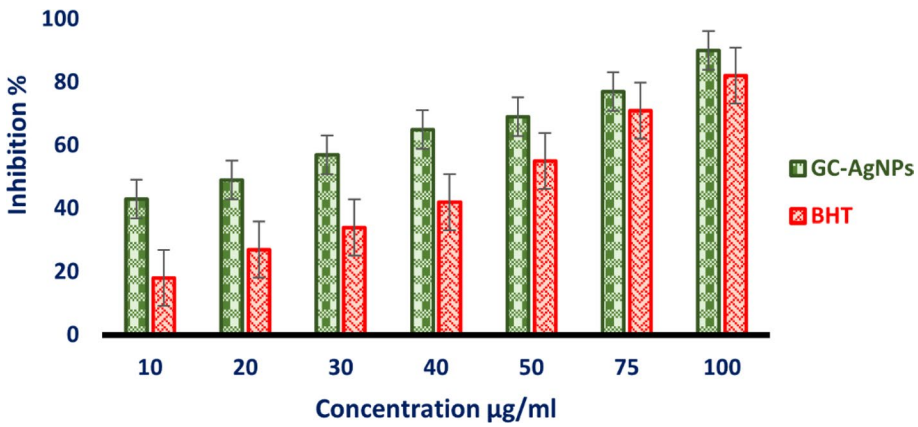

Fig. 11 The reducing power of the GC-AgNPs

Table 1 Antimicrobial activity of $AgNO_3$, and GC-AgNPs

Microorganisms	$AgNO_3$ 5 mg/mL	$AgNO_3$ 10 mg/mL	GC-AgNPs 5 mg/mL	GC-AgNPs 10 mg/mL	Standard antibiotics
Bacteria (mm)					Chloramphenicol (10 mg/mL)
Staphylococcus aureus	10.04 ± 0.39	11.72 ± 1.67	18.97 ± 0.47	20.65 ± 0.05	33.5 ± 0.20
Bacillus subtilis	–	–	15.08 ±	25.78 ± 0.38	34.2 ± 0.41
E. coli	13 ± 1.09	11 ± 0.85	23 ± 1.92	29.27 ± 0.75	29.05 ± 0.38
Pseudomonas aeruginosa	22.97 ± 2.45	26.00 ± 1.32	40.27 ± 0.56	38.03 ± 0.34	31.28 ± 0.94
Fungi (mm)					Nystatin (10 mg/mL)
Aspergillus flavus	13.45 ± 0.34	16.89 ± 0.40	18.34 ± 0.53	21.09 ± 0.71	22.45 ± 0.35
Aspergillus niger	14.30 ± 0.11	17.70 ± 0.35	18.20 ± 0.55	24.01 ± 0.65	21.04 ± 0.27
Aspergillus oryzae	9.66 ± 0.32	10.54 ± 0.27	13.42 ± 0.67	17.68 ± 0.35	25.03 ± 0.19
Penicillium camemberti	11.6 ± 0.61	13.21 ± 0.48	13.00 ± 0.38	15.03 ± 0.70	16.32 ± 0.82
Fusarium oxysporum	10.00 ± 0.53	10.47 ± 0.29	15.10 ± 0.11	16.23 ± 0.32	18.78 ± 0.38
Alternaria alterna	14.7 ± 0.18	15.66 ± 0.35	13.24 ± 0.76	16.31 ± 0.37	16.96 ± 0.21

All experimental values are represented as means ± SE of triplicates and resolved and analysed with the help of SPSS-17.0 software by one-way ANOVA and DMRT. The relationship is statistically significant when $P < 0.05$

GC-AgNPs goat colostrum mediated silver nanoparticles, *$AgNO_3$* silver nitrate, *ANOVA* analysis of variance, *DMRT* Duncan's new multiple range test, *SE* standard error, *SPSS* statistical package for the social sciences

were located at 29.27 mm and 25.78 mm in diameter. The minimum inhibition zone of 10.04 mm diameter was observed against *Staphylococcus aureus*.

Furthermore, in inhibition against *P. Aeruginosa*, the inhibitory zone of GC-AgNPs treatment (5 mg/mL) was observed with a 25.7 mm diameter in comparison to the 28.66 mm diameter of chloramphenicol (positive control). The chloramphenicol is reported to show inhibitory zones ranging from 24.00 to 33.66 mm against all bacteria. On the other hand, the inhibitory zones against the *P. aeruginosa* strain were observed in the range of 27.00–40.27 mm.

3.6.2.2 Disk Diffusion Antifungal Activity The global food scenario is directly affected by microbial spoilage of food, and the quality of the organoleptic products (aspect ratios, textures, taste, and aroma). The supreme ability of fungi to grow under any extreme conditions poses serious problems for the food chains [58]. Other than disturbing the food chain and its quality, some fungi (*Penicillium*, *Aspergillus*, *Alternaria*, and *Fusarium*) produce mycotoxins (secondary metabolites) to cause toxic effects not only in human beings but also in animals. According to a gross estimate, these mycotoxins contaminate nearly 25% of agricultural raw materials [59–61]. The aflatoxins and "ochratoxin A (OTA)" are the mycotoxins that trigger the food spoilage, and are produced by *Aspergillus* species, the "OTA" has also been produced by *Penicillium* species. *Aspergillus flavus* primarily produces aflatoxins which spoils various commodities of food [62]. There are some other mycotoxins like fumonisins and ochratoxins produced by *Aspergillus niger* present in grapes and coffee beans [63]. The fumonisins are also produced by *Penicillium camemberti* of mould-ripened cheese [64]; *Aspergillus oryzae* of soy sauce [65] or *Fusarium oxysporum* of infected bananas [66]. While the ochratoxins are produced by *Alternaria alterna* specie, present on fruit wounds [67]. Under these circumstances, the only solution to prevent food spoilage and losses is to control fungal contaminations at every niche of the food chain. The antifungal assay of GC-AgNPs against fungi, measured by inhibition zone diameter is summarized in Table 1. This treatment of GC-AgNPs (5 mg/mL) showed significant activities against *Penicillium camemberti* (13.00 mm), *Fusarium oxysporum* (15.10 mm), *Alternaria alterna* (13.24 mm), *Aspergillus oryzae* (13.42 mm), *Aspergillus niger* (17.02 mm) and *Aspergillus flavus* (18.34 mm).

In the $AgNO_3$ treatment (5 mg/mL), the inhibitory zones against various strains were observed as given here, against *Aspergillus flavus* (13.45 mm), *Fusarium oxysporum* (10.00 mm), against *Aspergillus oryzae* (9.66 mm), *Aspergillus niger* (14.30 mm) *Alternaria alterna* (14.7 mm) and against *Penicillium camemberti* zone was spotted at with a diameter of 11.6 mm. Panacek et al. [68] reported some exceptional antifungal properties of GC-AgNPs and the nanoparticles to serve as facilitators for trapping metal ions onto the surface of cells during extracellular synthesis and consequently reduce ions in the presence of enzymes.

There are three action mechanisms of silver nanoparticles: (1) Surface binding GC-AgNPs (with a diameter range of 1–10 nm) bind to the external surface of cell membranes and significantly impede the permeability and respiration; (2) The penetrating GC-AgNPs damage the bacterial cells probably by interacting with DNA and other sulfur and phosphorus containing compounds; (3) The release of potentially reactive silver ions by GC-AgNPs, may start reacting with the oppositely charged cell membranes.

3.6.2.3 Time Course Growth Activity The antimicrobial assay for GC-AgNPs was conducted against *E. coli*, *B. subtillis*, *L. monocytogenes*, *B. cereus*, *S. aureus*, *S. typhi*, and *C. albicans*, commonly found in food products [69]. These GC-AgNPs showed strong inhibition of food spoiling bacteria and the results of the treatment with GC-AgNPs (5 mg/mL) showed optical density (OD) of 0.47 against *B. subtillis* and 0.40 against *S. typhi* (Table 2). On the contrary, in the treatment with a higher concentration (10 mg/mL) of GC-AgNPs, greater inhibition was observed in bacterial strains [*E. coli* (0.38 OD); *L. monocytogenes* (0.29 OD); *B. cereus* (0.48 OD); *S. aureus* (0.45 OD); C. albicans (0.41 OD)]. All the bacterial strains were inhibited by the positive control and optical density in the range of 0.11–0.46 OD was observed.

There are many mechanistic arguments about the microbial growth inhibition by GC-AgNPs but the free radical generation mechanism is the most convincing and accepted one. The free radicals generated in the living systems, attack the membrane lipids to trigger their dissociation and ultimately inhibit microbial growth [70]. The silver ion (Ag^+) permeates into the bacteria through their cell wall [71], consequently, rupturing it and denaturing its protein to cause death. The positively charged silver ions which are relatively smaller than neutral GC-AgNPs can interact with electron-rich molecules present in the bacterial cell wall having sulphur, nitrogen, or phosphorous. The generation of silver ions by the oxidation of elemental silver requires some oxidizing agents. The antibacterial potential of the GC-AgNPs is ascribed to their attachment to the cell membrane surface, thus hampering cell permeation and respiration [72]. It is also reported that silver nanoparticles inhibit cell proliferation by attaching to the enzymes or DNA [73].

3.6.2.4 Broth Dilution (BD) Method BD method has the advantage over disc diffusion assay, as it is a direct contact test and independent of diffusion properties. The antimicrobial activity of GC-AgNPs in terms of MIC, MBC, and MFC is presented in Table 3. Among bacterial pathogens, maximum sensitivity was shown in *E. coli* and the least sen-

Table 2 Antibacterial activity of GC-AgNPs

Samples and bacterial strains	Time course growth assay (OD 550 nm) Inhibition of bacterial growth at time intervals				
	0 h	1 h	2 h	3 h	5 h
GC-AgNPs (5 mg/mL)					
E. coli	0.22 ± 0.02	0.27 ± 0.00	0.28 ± 0.02	0.29 ± 0.01	0.32 ± 0.02
B. Subtillis	0.26 ± 0.00	0.27 ± 0.00	0.27 ± 0.02	0.29 ± 0.00	0.47 ± 0.00
L. monocytogenes	0.16 ± 0.01	0.18 ± 0.01	0.19 ± 0.01	0.20 ± 0.02	0.28 ± 0.00
B. cereus	0.19 ± 0.01	0.21 ± 0.01	0.21 ± 0.01	0.24 ± 0.01	0.30 ± 0.03
S. aureus	0.25 ± 0.00	0.30 ± 0.02	0.30 ± 0.01	0.32 ± 0.02	0.37 ± 0.01
S. typhi	0.21 ± 0.02	0.24 ± 0.01	0.25 ± 0.02	0.26 ± 0.02	0.40 ± 0.02
C. Albicans	0.18 ± 0.01	0.19 ± 0.02	0.20 ± 0.01	0.22 ± 0.02	0.25 ± 0.01
GC-AgNPs (10 mg/mL)					
E. coli	0.26 ± 0.01	0.27 ± 0.01	0.27 ± 0.01	0.30 ± 0.02	0.38 ± 0.00
B. Subtillis	0.20 ± 0.02	0.22 ± 0.02	0.24 ± 0.00	0.27 ± 0.00	0.40 ± 0.02
L. monocytogenes	0.17 ± 0.00	0.18 ± 0.02	0.19 ± 0.02	0.20 ± 0.02	0.29 ± 0.00
B. cereus	0.24 ± 0.00	0.26 ± 0.00	0.29 ± 0.00	0.32 ± 0.01	0.48 ± 0.03
S. aureus	0.21 ± 0.02	0.22 ± 0.01	0.25 ± 0.02	0.25 ± 0.02	0.45 ± 0.02
S. typhi	0.19 ± 0.01	0.20 ± 0.02	0.21 ± 0.01	0.23 ± 0.00	0.36 ± 0.00
C. Albicans	0.27 ± 0.00	0.27 ± 0.02	0.28 ± 0.01	0.29 ± 0.01	0.41 ± 0.04
$AgNO_3$ (5 mg/mL)					
E. coli	0.20 ± 0.01	0.22 ± 0.01	0.23 ± 0.02	0.25 ± 0.01	0.32 ± 0.01
B. Subtillis	0.19 ± 0.02	0.20 ± 0.01	0.20 ± 0.01	0.23 ± 0.02	0.30 ± 0.00
L. monocytogenes	0.14 ± 0.01	0.15 ± 0.01	0.16 ± 0.00	0.18 ± 0.00	0.19 ± 0.03
B. cereus	0.19 ± 0.02	0.20 ± 0.01	0.20 ± 0.01	0.21 ± 0.01	0.26 ± 0.02
S. aureus	0.24 ± 0.01	0.26 ± 0.01	0.28 ± 0.01	0.30 ± 0.02	0.35 ± 0.00
S. typhi	0.19 ± 0.03	0.20 ± 0.01	0.21 ± 0.01	0.28 ± 0.02	0.34 ± 0.02
C. Albicans	0.16 ± 0.01	0.16 ± 0.00	0.17 ± 0.01	0.19 ± 0.00	0.28 ± 0.01
$AgNO_3$ (10 mg/mL)					
E. coli	0.25 ± 0.02	0.26 ± 0.03	0.31 ± 0.00	0.32 ± 0.01	0.40 ± 0.01
B. Subtillis	0.29 ± 0.02	0.30 ± 0.02	0.33 ± 0.01	0.39 ± 0.02	0.44 ± 0.02
L. monocytogenes	0.17 ± 0.01	0.18 ± 0.01	0.20 ± 0.02	0.20 ± 0.01	0.23 ± 0.01
B. cereus	0.20 ± 0.00	0.22 ± 0.02	0.23 ± 0.01	0.24 ± 0.00	0.27 ± 0.01
S. aureus	0.21 ± 0.01	0.22 ± 0.00	0.24 ± 0.00	0.26 ± 0.01	0.33 ± 0.00
S. typhi	0.22 ± 0.00	0.25 ± 0.03	0.26 ± 0.02	0.29 ± 0.00	0.35 ± 0.02
C. Albicans	0.35 ± 0.01	0.36 ± 0.00	0.36 ± 0.01	0.37 ± 0.02	0.39 ± 0.00
Chloramphenicol (10 mg/mL)					
E. coli	0.15 ± 0.01	0.15 ± 0.01	0.16 ± 0.02	0.17 ± 0.01	0.18 ± 0.00
B. Subtillis	0.19 ± 0.01	0.20 ± 0.01	0.22 ± 0.01	0.22 ± 0.01	0.25 ± 0.00
L. monocytogenes	0.13 ± 0.02	0.13 ± 0.01	0.14 ± 0.05	0.15 ± 0.02	0.17 ± 0.02
B. cereus	0.25 ± 0.01	0.27 ± 0.04	0.27 ± 0.02	0.32 ± 0.01	0.47 ± 0.01
S. aureus	0.36 ± 0.01	0.38 ± 0.02	0.39 ± 0.04	0.40 ± 0.01	0.54 ± 0.02
S. typhi	0.19 ± 0.02	0.19 ± 0.01	0.21 ± 0.00	0.23 ± 0.03	0.33 ± 0.01
C. Albicans	0.13 ± 0.01	0.14 ± 0.02	0.15 ± 0.02	0.15 ± 0.01	0.19 ± 0.01

All values represented as mean ± SE of triplicate values and analysed using SPSS 17.0 software with one-way ANOVA followed by DMRT and their relationship was statistically significant when $P < 0.05$

GC-AgNPs goat colostrum mediated silver nanoparticles, *$AgNO_3$* silver nitrate, *ANOVA* analysis of variance, *DMRT* Duncan's new multiple range test, *SE* standard error, *SPSS* statistical package for the social sciences, *OD* optical density

sitivity was observed in *B. Subtilis* [74]. *C. albicans* showed higher sensitivity to GC-AgNPs than *A. Niger*. The MIC and MBC/MFC values are much less than the reported one, indicating the high potency of GC-AgNPs. The higher MIC and MBC value of gram-positive *B. subtilis* may be due to the thick peptidoglycan layer that resists the penetration of GC-

Table 3 MIC, MBC and MFC of GC-AgNPs

Microorganisms	GC-AgNPs (µg/mL)		AgNPs (µg/mL)
Bacteria	MIC	MBC	MIC (literature)
E. coli	15 ± 0.1	15 ± 0.3	75 ± 0.5 [75]
S. typhi	25 ± 0.3	25 ± 0.5	75 ± 0.2 [76]
B. subtilis	30 ± 0.1	30 ± 0.4	70 ± 0.3 [75]
Fungi	MIC	MFC	MIC (literature)
C. albicans	40 ± 0.2	40 ± 0.6	500 ± 0.1 [77]
A. niger	100 ± 0.3	100 ± 0.4	75 ± 0.1 [78]

Table 4 Anti-inflammatory activity of GC-AgNPs

Sample	Concentration (mg/mL)	Optical density	% inhibition
Control	–	2.53 ± 0.02	–
GC-AgNps	0.025	0.22 ± 0.01***	92.45
	0.05	0.14 ± 0.02***	96.34
	0.1	0.08 ± 0.00***	98.01
	0.2	0.04 ± 0.01***	98.90
	0.4	0.12 ± 0.01	96.75
Acetylsalicylic acid	5	0.91 ± 0.05***	67.31
	10	1.18 ± 0.07***	54.48
	15	1.30 ± 0.10**	51.76
	25	1.56 ± 0.23**	47.39
	50	2.0 ± 0.09	30.54
	100	2.31 ± 0.01	14.30

The results are expressed as means ± SEM in each group (n = 3); ** P 0.01, *** P 0.001 compared to controls

AgNPs through the cell membrane. The higher MIC and MFC value of *A. niger* than *C. albicans* may be linked to the spore-producing and filamentous nature of fungi causing a decrease in the sensitivity.

3.6.3 Anti-inflammatory Activity

The *in-vitro* bioassay of silver nanoparticles against albumin denaturation to assess their antiarthritic effect is summarized in Table 4. There was significant inhibition of egg albumin denaturation at concentrations ($P < 0.001$), but the highest inhibition percentage of GC-AgNPs (99.2%) was obtained at 0.2 mg/mL. Whereas the standard drug (acetylsalicylic acid) exhibited comparatively less inhibition (71%) even at a higher concentration (5 mg/mL) than nanoparticles.

The involvement of protein denaturation in arthritic reactions and tissue damage during inflammations is well documented [79, 80]. It is concluded that the synthesized GC-AgNPs have effective inhibition of thermally induced denaturation of albumin at all concentrations; hence they control the protein denaturation during inflammations. It is also considered that GC-AgNPs can interrupt the release mediators or antagonize their actions during acute inflammations.

3.6.4 Biocompatibility Study

The synthesized GC-AgNPs could be implicated successfully in the biomedical science and food industry only after recognizing their biocompatibility potential. The

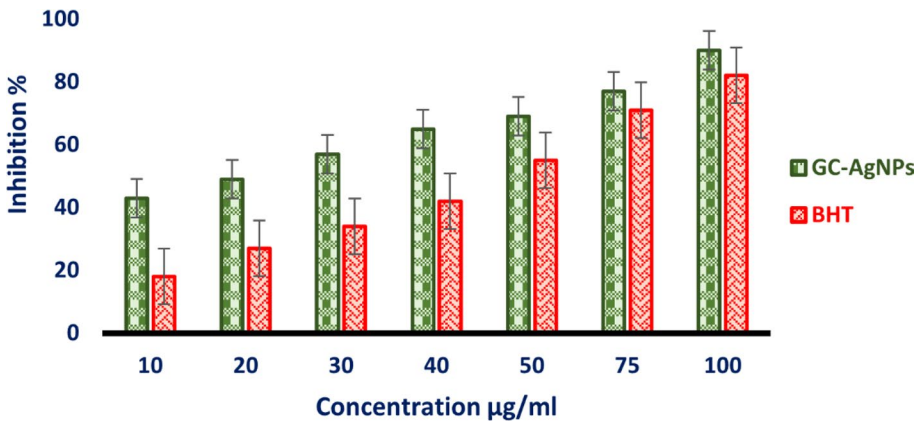

Fig. 12 Cytotoxicity study of GC-AgNPs on the human cell line. The percentage of cell viability is represented as the mean ± SD ($n = 3$). The control was considered 100% viable in all experiments. Bars having different superscripts were significantly different from each other ($P < 0.05$), whereas the bars having the same superscripts ($P > 0.05$) were not significantly different from each other

biocompatibility of the GC-AgNPs was evaluated from their cytotoxicity to normal fibroblast cell lines (L-929). The inhibitory potential of the GC-AgNPs against L-929 was observed at low concentrations during this study. The viability of the normal fibroblast cells declined with the increasing concentration of the GC-AgNPs (Fig. 12). The IC_{50} value of 615 ± 0.64 mg/mL against normal cell lines indicates the significant biocompatibility and safety of GC-AgNPs for the human body. Fortunately, our present findings are corroborated with previously reported findings [81]. The thorough implementation and practical application of GC-AgNPs as a product require comprehensive studies on their biocompatibility and biosafety.

4 Conclusion

The antimicrobial nanoparticles play a vital and critical role in the quality and shelf life of food. In this context, we successfully report an ecological and cost-effective methodology for synthesising the silver nanoparticle mediated by goat colostrum. GC-AgNPs have an average size of 6.93 nm. The characterization results show that goat colostrum is suitable for the low-cost synthesis of silver nanoparticles. GC-AgNPs possess excellent antimicrobial properties against six foodborne pathogens. In addition to this, the inflammatory and antioxidant activity of the GC-AgNPs confirmed their prevention from oxidation due to radical activity as well as other factors. Cytotoxicity results revealed that they are highly biocompatible to human fibroblast cell lines (L-929). Because of the non-toxic nature of goat colostrum, antimicrobial GC-AgNPs have great potential in medical science and the current study recommends strong participation of nanoscience against foodborne pathogens.

Supplementary Information The online version contains supplementary material available at https://doi.org/10.1007/s42250-022-00402-8.

Acknowledgements The authors gratefully acknowledge and appreciate valuable contributions from the Department of Chemistry, The Islamia University Bahawalpur, Pakistan, Department of Biochemistry, College of Science, University of Jeddah, Saudi Arabia in providing every possible support to carry out this work.

Author Contributions MBT, MS; Conceptualization, supervision, and editing. MBT, WA, AR; methodology and writing. RMA, AMA, AMB; Biological analysis. SS, RHA, MS; review and editing, HFA, SN; Data curation. All authors have read and agreed to the manuscript.

Declarations

Conflict of interest No conflict of interest is present among the authors of this manuscript.

References

1. Dubey SP, Lahtinen M, Sillanpää M (2010) Green synthesis and characterizations of silver and gold nanoparticles using leaf extract of *Rosa rugosa*. Colloids Surf A 364(1–3):34–41
2. Ahmad F, Taj MB, Ramzan M, Raheel A, Shabbir S, Imran M, Iqbal HM (2020) *Flacourtia indica* based biogenic nanoparticles: development, characterization, and bioactivity against wound associated pathogens. Mater Res Exp 7(1):015026
3. Ayati A, Ahmadpour A, Bamoharram FF, Heravi MM, Sillanpää M (2012) Rate redox-controlled green photosynthesis of gold nanoparticles using $H_{3+x}PMo_{12-x}V_xO$ 40. Gold Bull 45(3):145–151
4. Singh SP, Bhargava C, Dubey V, Mishra A, Singh Y (2017) Silver nanoparticles: biomedical applications, toxicity, and safety issues. In J Res Pharm Pharm Sci 4(2):01–10
5. Mallikarjuna K, Narasimha G, Dillip G, Praveen B, Shreedhar B, Lakshmi CS, Reddy B, Raju BDP (2011) Green synthesis of silver nanoparticles using *Ocimum* leaf extract and their characterization. Dig J Nanomater Biostruct 6(1):181–186
6. Dubey SP, Lahtinen M, Sillanpää M (2010) Tansy fruit mediated greener synthesis of silver and gold nanoparticles. Process Biochem 45(7):1065–1071
7. Ahmadpour A, Tanhaei B, Bamoharram F, Ayati A, Sillanpaa M (2012) Green, rapid and facile HPMo-assisted synthesis of silver nanoparticles. Curr Nanosci 8(6):880–884
8. Dubey SP, Dwivedi AD, Lahtinen M, Lee C, Kwon Y-N, Sillanpaa M (2013) Protocol for development of various plants leaves extract in single-pot synthesis of metal nanoparticles. Spectrochim Acta Part A Mol Biomol Spectrosc 103:134–142
9. Thakkar KN, Mhatre SS, Parikh RY (2010) Biological synthesis of metallic nanoparticles. Nanomed Nanotechnol Biol Med 6(2):257–262
10. Zaheer Z (2012) Silver nanoparticles to self-assembled films: green synthesis and characterization. Colloids Surf B 90:48–52
11. Singh J, Kumar V, Jolly SS, Kim K-H, Rawat M, Kukkar D, Tsang YF (2019) Biogenic synthesis of silver nanoparticles and its photocatalytic applications for removal of organic pollutants in water. J Ind Eng Chem 80:247–257
12. Ajayi A, Larayetan R, Yahaya A, Falola OO, Ude NA, Adamu H, Oguche SM, Abraham K, Egbagba AO, Egwumah C (2021) Biogenic synthesis of silver nanoparticles with bitter leaf (*Vernonia amygdalina*) aqueous extract and its effects on testosterone-induced benign prostatic hyperplasia (BPH) in wistar rat. Chem Afr 4(4):791–807
13. Bhat M, Chakraborty B, Kumar RS, Almansour AI, Arumugam N, Kotresha D, Pallavi S, Dhanyakumara S, Shashiraj K, Nayaka S (2021) Biogenic synthesis, characterization and antimicrobial activity of *Ixora brachypoda* (DC) leaf extract mediated silver nanoparticles. J King Saud Univ Sci 33(2):101296
14. Akwu NA, Naidoo Y, Singh M, Nundkumar N, Daniels A, Lin J (2021) Two temperatures biogenic synthesis of silver nanoparticles from *Grewia lasiocarpa* E. Mey. ex Harv. leaf and stem bark extracts: characterization and applications. BioNanoScience 11(1):142–158
15. Khan AA, Alanazi AM, Alsaif N, Wani TA, Bhat MA (2021) Pomegranate peel induced biogenic synthesis of silver nanoparticles and their multifaceted potential against intracellular pathogen and cancer. Saudi J Biol Sci 28(8):4191–4200
16. Hiba H, Thoppil JE (2022) Medicinal herbs as a panacea for biogenic silver nanoparticles. Bull Natl Res Centre 46(1):1–15
17. Gul AR, Shaheen F, Rafique R, Bal J, Waseem S, Park TJ (2021) Grass-mediated biogenic synthesis of silver nanoparticles and their drug delivery evaluation: a biocompatible anti-cancer therapy. Chem Eng J 407:127202

18. Kanimozhi S, Durga R, Sabithasree M, Kumar AV, Sofiavizhimalar A, Kadam AA, Rajagopal R, Sathya R, Azelee NIW (2022) Biogenic synthesis of silver nanoparticle using *Cissus quadrangularis* extract and its invitro study. J King Saud Univ Sci 34(4):101930
19. Raj S, Trivedi R, Soni V (2021) Biogenic synthesis of silver nanoparticles, characterization and their applications—a review. Surfaces 5(1):67–90
20. Ahmad F, Taj MB, Ramzan M, Ali H, Ali A, Adeel M, Iqbal HM, Imran M (2020) One-pot synthesis and characterization of in-house engineered silver nanoparticles from *Flacourtia jangomas* fruit extract with effective antibacterial profiles. J Nanostruct Chem 11:1–11
21. Kuppurangan G, Karuppasamy B, Nagarajan K, Sekar RK, Viswaprakash N, Ramasamy T (2016) Biogenic synthesis and spectroscopic characterization of silver nanoparticles using leaf extract of *Indoneesiella echioides*: in vitro assessment on antioxidant, antimicrobial and cytotoxicity potential. Appl Nanosci 6(7):973–982
22. Njagi EC, Huang H, Stafford L, Genuino H, Galindo HM, Collins JB, Hoag GE, Suib SL (2011) Biosynthesis of iron and silver nanoparticles at room temperature using aqueous sorghum bran extracts. Langmuir 27(1):264–271
23. Lengke MF, Fleet ME, Southam G (2007) Biosynthesis of silver nanoparticles by filamentous cyanobacteria from a silver(I) nitrate complex. Langmuir 23(5):2694–2699
24. Jha D, Thiruveedula PK, Pathak R, Kumar B, Gautam HK, Agnihotri S, Sharma AK, Kumar P (2017) Multifunctional biosynthesized silver nanoparticles exhibiting excellent antimicrobial potential against multi-drug resistant microbes along with remarkable anticancerous properties. Mater Sci Eng C 80:659–669
25. Anandalakshmi K, Venugobal J, Ramasamy V (2016) Characterization of silver nanoparticles by green synthesis method using *Pedalium murex* leaf extract and their antibacterial activity. Appl Nanosci 6(3):399–408
26. Behravan M, Panahi AH, Naghizadeh A, Ziaee M, Mahdavi R, Mirzapour A (2019) Facile green synthesis of silver nanoparticles using *Berberis vulgaris* leaf and root aqueous extract and its antibacterial activity. Int J Biol Macromol 124:148–154
27. Siddiqi KS, Husen A, Rao RA (2018) A review on biosynthesis of silver nanoparticles and their biocidal properties. J Nanobiotechnol 16(1):14
28. Athreya AG, Shareef MI, Gopinath S (2019) Antibacterial activity of silver nanoparticles isolated from cow's milk, hen's egg white and lysozyme: a comparative study. Arab J Sci Eng 44(7):6231–6240
29. Pandey S, Klerk CD, Kim J, Kang M, Fosso-Kankeu E (2020) Eco friendly approach for synthesis, characterization and biological activities of milk protein stabilized silver nanoparticles. Polymers 12(6):1418
30. Walstra P (1999) Dairy technology: principles of milk properties and processes. CRC Press, New York
31. Lee K-J, Park S-H, Govarthanan M, Hwang P-H, Seo Y-S, Cho M, Lee W-H, Lee J-Y, Kamala-Kannan S, Oh B-T (2013) Synthesis of silver nanoparticles using cow milk and their antifungal activity against phytopathogens. Mater Lett 105:128–131
32. Hegazi A, Elshazly EH, Abdou AM, Abd Allah F, Abdel-Rahman EH (2014) Potential antibacterial properties of silver nanoparticles conjugated with cow and camel milks. Glob Vet 12:745–749
33. Fischer-Tlustos A, Hertogs K, van Niekerk J, Nagorske M, Haines D, Steele M (2020) Oligosaccharide concentrations in colostrum, transition milk, and mature milk of primi-and multiparous Holstein cows during the first week of lactation. J Dairy Sci 103(4):3683–3695
34. Varadharaj V, Ramaswamy A, Sakthivel R, Subbaiya R, Barabadi H, Chandrasekaran M, Saravanan M (2019) Antidiabetic and antioxidant activity of green synthesized starch nanoparticles: an in vitro study. J Clust Sci 178:1–10
35. Alavi M, Karimi N (2018) Characterization, antibacterial, total antioxidant, scavenging, reducing power and ion chelating activities of green synthesized silver, copper and titanium dioxide nanoparticles using *Artemisia haussknechtii* leaf extract. Artif Cells Nanomed Biotechnol 46(8):2066–2081
36. Yarrappagaari S, Gutha R, Narayanaswamy L, Thopireddy L, Benne L, Mohiyuddin SS, Vijayakumar V, Saddala RR (2020) Eco-friendly synthesis of silver nanoparticles from the whole plant of *Cleome viscosa* and evaluation of their characterization, antibacterial, antioxidant and antidiabetic properties. Saudi J Biol Sci 27(12):3601–3614
37. Baskaran X, Vigila AVG, Parimelazhagan T, Muralidhara-Rao D, Zhang S (2016) Biosynthesis, characterization, and evaluation of bioactivities of leaf extract-mediated biocompatible silver nanoparticles from an early tracheophyte, *Pteris tripartita* sw. Int J Nanomed 11:5789
38. Bhakya S, Muthukrishnan S, Sukumaran M, Muthukumar M (2016) Biogenic synthesis of silver nanoparticles and their antioxidant and antibacterial activity. Appl Nanosci 6(5):755–766
39. Sousa A, Ferreira IC, Barros L, Bento A, Pereira JA (2008) Effect of solvent and extraction temperatures on the antioxidant potential of traditional stoned table olives "alcaparras." LWT Food Sci Technol 41(4):739–745
40. Patil S, Rajiv P, Sivaraj R (2015) An investigation of antioxidant and cytotoxic properties of green synthesized silver nanoparticles. Indo Am J Pharm Sci 2(10):1453–1459
41. Dogra V, Kaur G, Jindal S, Kumar R, Kumar S, Singhal NK (2019) Bactericidal effects of metallosurfactants based cobalt oxide/hydroxide nanoparticles against *Staphylococcus aureus*. Sci Total Environ 681:350–364
42. Bocate KP, Reis GF, de Souza PC, Junior AGO, Durán N, Nakazato G, Furlaneto MC, de Almeida RS, Panagio LA (2019) Antifungal activity of silver nanoparticles and simvastatin against toxigenic species of *Aspergillus*. Int J Food Microbiol 291:79–86
43. Rajeshkumar S, Malarkodi C (2014) In vitro antibacterial activity and mechanism of silver nanoparticles against foodborne pathogens. Bioinorgchem Appl 2014:581890
44. Chan S, Don M (2012) Characterization of Ag nanoparticles produced by white-rot fungi and its in vitro antimicrobial activities. Int Arab J Antimicrob Agents 2(33):1–8
45. Gunalan S, Sivaraj R, Rajendran V (2012) Green synthesized ZnO nanoparticles against bacterial and fungal pathogens. Prog Nat Sci Mater Int 22(6):693–700
46. Meva FE, Mbeng JOA, Ebongue CO, Schlüsener C, Kökçam-Demir Ü, Ntoumba AA, Kedi PBE, Elanga E, Loudang E-RN, Nko'o MHJ (2019) Stachytarpheta cayennensis aqueous extract, a new bioreactor towards silver nanoparticles for biomedical applications. J Biomater Nanobiotechnol 10(02):102
47. Shanmuganathan R, Karuppusamy I, Saravanan M, Muthukumar H, Ponnuchamy K, Ramkumar VS, Pugazhendhi A (2019) Synthesis of silver nanoparticles and their biomedical applications—a comprehensive review. Curr Pharm Des 25(24):2650–2660
48. Wiley BJ, Im SH, Li Z-Y, McLellan J, Siekkinen A, Xia Y (2006) Maneuvering the surface plasmon resonance of silver nanostructures through shape-controlled synthesis. ACS Publications, Washington
49. Ye X, Jin L, Caglayan H, Chen J, Xing G, Zheng C, Doan-Nguyen V, Kang Y, Engheta N, Kagan CR (2012) Improved size-tunable synthesis of monodisperse gold nanorods through the use of aromatic additives. ACS Nano 6(3):2804–2817
50. Mehdizadeh S, Ghasemi N, Ramezani M (2019) The synthesis of silver nanoparticles using beetroot extract and its antibacterial and catalytic activity. Iran Chem Commun 7:655–668

51. Lakkim V, Reddy MC, Pallavali RR, Reddy KR, Reddy CV, Bilgrami AL, Lomada D (2020) Green synthesis of silver nanoparticles and evaluation of their antibacterial activity against multidrug-resistant bacteria and wound healing efficacy using a murine model. Antibiotics 9(12):902
52. Arshad H, Sadaf S, Hassan U (2022) De-novo fabrication of sunlight irradiated silver nanoparticles and their efficacy against *E. coli* and *S. epidermidis*. Sci Rep 12(1):1–10
53. Nguyen VT (2020) Sunlight-driven synthesis of silver nanoparticles using pomelo peel extract and antibacterial testing. J Chem 2020:1–9
54. Sadeghzadeh SM, Zhiani R, Emrani S (2017) KCC-1/GMSI/VB12 as a new nano catalyst for the carbonylative Suzuki-Miyaura crosscoupling reaction. RSC Adv 7(51):32139–32145
55. Gharagozlou M, Naghibi S (2015) Preparation of vitamin B12–TiO2 nanohybrid studied by TEM, FTIR and optical analysis techniques. Mater Sci Semicond Process 35:166–173
56. Shameli K, Ahmad MB, Zamanian A, Sangpour P, Shabanzadeh P, Abdollahi Y, Zargar M (2012) Green biosynthesis of silver nanoparticles using Curcuma longa tuber powder. Int J Nanomed 7:5603
57. Malassis L, Dreyfus R, Murphy RJ, Hough LA, Donnio B, Murray CB (2016) One-step green synthesis of gold and silver nanoparticles with ascorbic acid and their versatile surface post-functionalization. RSC Adv 6(39):33092–33100
58. Paterson RRM, Lima N (2010) How will climate change affect mycotoxins in food? Food Res Int 43(7):1902–1914
59. García-Cela E, Ramos A, Sanchis V, Marin S (2012) Emerging risk management metrics in food safety: FSO, PO. How do they apply to the mycotoxin hazard? Food Control 25(2):797–808
60. Suleiman RA, Kurt RA (2015) Current maize production, postharvest losses and the risk of mycotoxins contamination in Tanzania. In: 2015 ASABE annual international meeting. American Society of Agricultural and Biological Engineers, p 1.
61. Jard G, Liboz T, Mathieu F, Guyonvarc'h A, Lebrihi A (2011) Review of mycotoxin reduction in food and feed: from prevention in the field to detoxification by adsorption or transformation. Food Addit Contam Part A 28(11):1590–1609
62. Barkai-Golan R, Paster N (2008) Mouldy fruits and vegetables as a source of mycotoxins: part 1. World Mycotoxin J 1(2):147–159
63. Perrone G, Susca A, Cozzi G, Ehrlich K, Varga J, Frisvad JC, Meijer M, Noonim P, Mahakarnchanakul W, Samson RA (2007) Biodiversity of Aspergillus species in some important agricultural products. Stud Mycol 59:53–66
64. Delgado J, Peromingo B, Nunez F, Asensio MA (2016) Use of molds and their antifungal proteins for biocontrol of toxigenic molds on dry-ripened cheese and meats. Curr Opin Food Sci 11:40–45
65. Liang Y, Pan L, Lin Y (2009) Analysis of extracellular proteins of *Aspergillus oryzae* grown on soy sauce koji. Biosci Biotechnol Biochem 73:192–195
66. Li C, Chen S, Zuo C, Sun Q, Ye Q, Yi G, Huang B (2011) The use of GFP-transformed isolates to study infection of banana with *Fusarium oxysporum* f. sp. *cubense* race 4. Eur J Plant Pathol 131(2):327–340
67. Mahmoudi E, Ahmadi A, Naderi D (2012) Effect of *Zataria multiflora* essential oil on *Alternaria alternata* in vitro and in an assay on tomato fruits. J Plant Dis Prot 119(2):53–58
68. Panáček A, Kolář M, Večeřová R, Prucek R, Soukupova J, Kryštof V, Hamal P, Zbořil R, Kvítek L (2009) Antifungal activity of silver nanoparticles against *Candida* spp. Biomaterials 30(31):6333–6340
69. Puišo J, Jonkuvienė D, Mačionienė I, Šalomskienė J, Jasutienė I, Kondrotas R (2014) Biosynthesis of silver nanoparticles using lingonberry and cranberry juices and their antimicrobial activity. Colloids Surf, B 121:214–221
70. Wang L, Hu C, Shao L (2017) The antimicrobial activity of nanoparticles: present situation and prospects for the future. Int J Nanomed 12:1227
71. Rawashdeh R, Haik Y (2009) Antibacterial mechanisms of metallic nanoparticles: a review. Dyn Biochem Process Biotechnol Mol Biol 3(2):12–20
72. Franci G, Falanga A, Galdiero S, Palomba L, Rai M, Morelli G, Galdiero M (2015) Silver nanoparticles as potential antibacterial agents. Molecules 20(5):8856–8874
73. Shankar SS, Rai A, Ahmad A, Sastry M (2004) Rapid synthesis of Au, Ag, and bimetallic Au core–Ag shell nanoparticles using neem (*Azadirachta indica*) leaf broth. J Colloid Interface Sci 275(2):496–502
74. Arokiyaraj S, Arasu MV, Vincent S, Prakash NU, Choi SH, Oh Y-K, Choi KC, Kim KH (2014) Rapid green synthesis of silver nanoparticles from *Chrysanthemum indicum* L and its antibacterial and cytotoxic effects: an in vitro study. Int J Nanomed 9:379
75. Morones JR, Elechiguerra JL, Camacho A, Holt K, Kouri JB, Ramírez JT, Yacaman MJ (2005) The bactericidal effect of silver nanoparticles. Nanotechnology 16(10):2346
76. Chandrakanth RK, Ashajyothi C, Oli AK, Prabhurajeshwar C (2014) Potential bactericidal effect of silver nanoparticles synthesised from Enterococcus species. Orient J Chem 30:1253–1262
77. Nasrollahi A, Pourshamsian K, Mansourkiaee P (2011) Antifungal activity of silver nanoparticles on some of fungi. Int J Nano Dimension 1(3):233–239
78. Jain J, Arora S, Rajwade JM, Omray P, Khandelwal S, Paknikar KM (2009) Silver nanoparticles in therapeutics: development of an antimicrobial gel formulation for topical use. Mol Pharm 6(5):1388–1401
79. Govindappa M, Hemashekhar B, Arthikala M-K, Rai VR, Ramachandra Y (2018) Characterization, antibacterial, antioxidant, antidiabetic, anti-inflammatory and antityrosinase activity of green synthesized silver nanoparticles using *Calophyllum tomentosum* leaves extract. Results Phys 9:400–408
80. Aafreen MM, Anitha R, Preethi RC, Rajeshkumar S, Lakshmi T (2019) Anti-Inflammatory activity of silver nanoparticles prepared from ginger oil—an invitro approach. Indian J Public Health Res Dev 10(7):145–145
81. Netala VR, Bethu MS, Pushpalatha B, Baki VB, Aishwarya S, Rao JV, Tartte V (2016) Biogenesis of silver nanoparticles using endophytic fungus *Pestalotiopsis microspora* and evaluation of their antioxidant and anticancer activities. Int J Nanomed 11:5683